Cancer Cell, Volume *35*

Supplemental Information

BCL2 Amplicon Loss and Transcriptional Remodeling Drives ABT-199 Resistance in B Cell Lymphoma Models

Xiaohong Zhao, Yuan Ren, Matthew Lawlor, Bijal D. Shah, Paul M.C. Park, Tint Lwin, Xuefeng Wang, Kenian Liu, Michelle Wang, Jing Gao, Tao Li, Mousheng Xu, Ariosto S. Silva, Kaplan Lee, Tinghu Zhang, John M. Koomen, Huijuan Jiang, Praneeth R. Sudalagunta, Mark B. Meads, Fengdong Cheng, Chengfeng Bi, Kai Fu, Huitao Fan, William S. Dalton, Lynn C. Moscinski, Kenneth H. Shain, Eduardo M. Sotomayor, Gang Greg Wang, Nathanael S. Gray, John L. Cleveland, Jun Qi, and Jianguo Tao

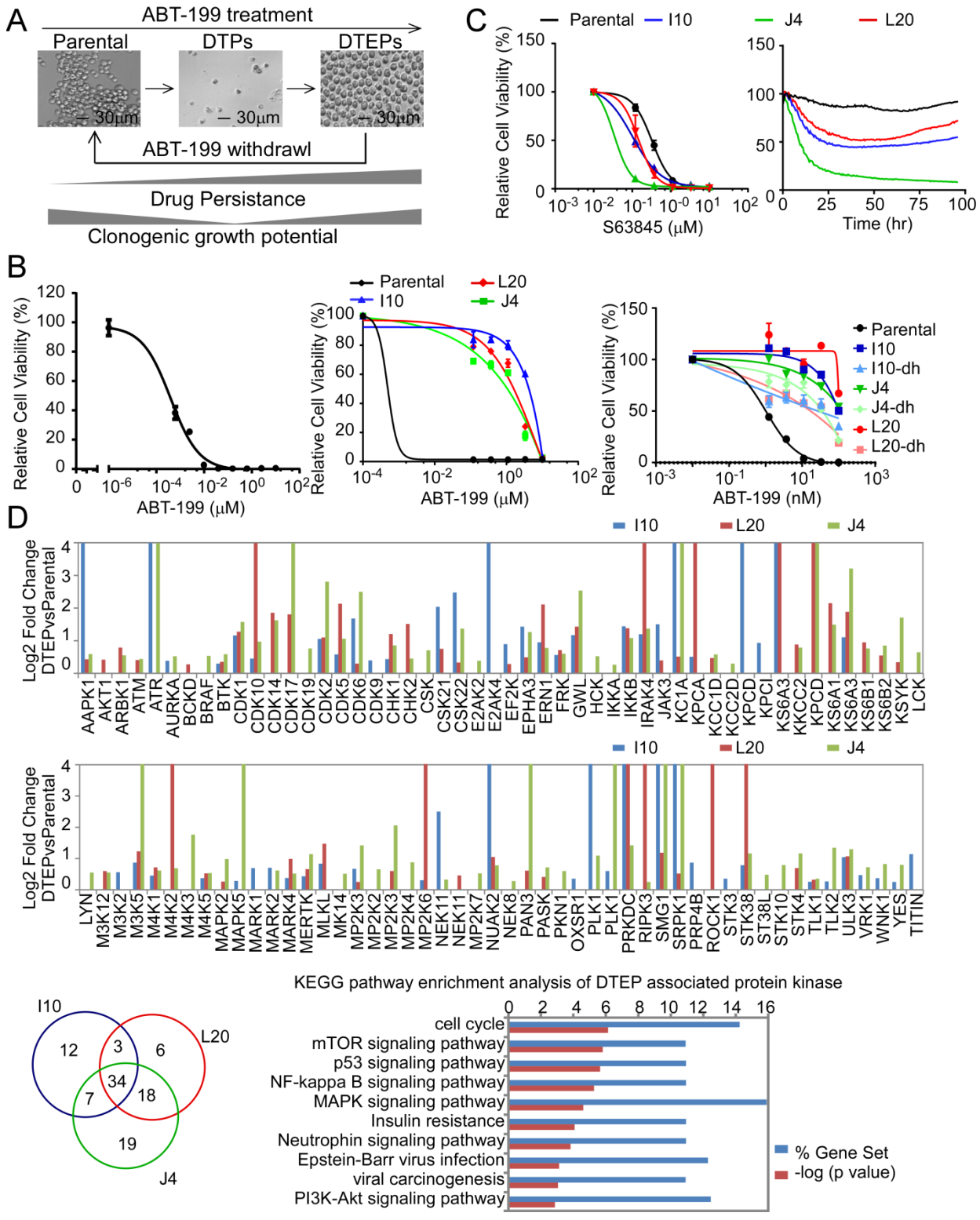
A
ABT-199 treatment
Parental
DTPs
DTEPs
~ 30μm
~ 30μm
~ 30μm
ABT-199 withdrawl
Drug Persistance
Clonogenic growth potential
C
Parental
I10
J4
L20
Relative Cell Viability (%)
S63845 (μM)
Time (hr)
B
Relative Cell Viability (%)
ABT-199 (μM)
Parental
I10
J4
L20
ABT-199 (μM)
Parental
I10
I10-dh
J4
J4-dh
L20
L20-dh
ABT-199 (nM)
D
I10
L20
J4
Log2 Fold Change DTEPvsParental
AAPK1 AKT1 ARBK1 ATM ATR AURKA BCKD BRAF BTK CDK1 CDK10 CDK14 CDK17 CDK19 CDK2 CDK5 CDK6 CDK9 CHK1 CHK2 CSK CSK21 CSK22 E2AK2 E2AK4 EF2K EPHA3 ERN1 FRK GWL HCK IKKA IKKB IRAK4 JAK3 KC1A KPCA KCC1D KCC2D KPCD KPCI KS6A3 KKCC2 KPCD KS6A1 KS6A3 KS6B1 KS6B2 KSYK LCK
I10
L20
J4
Log2 Fold Change DTEPvsParental
LYN M3K12 M3K2 M3K5 M4K1 M4K2 M4K3 M4K5 MAPK2 MAPK5 MARK1 MARK2 MARK4 MERTK MLKL MK14 MP2K3 MP2K2 MP2K3 MP2K4 MP2K6 NEK11 NEK11 MP2K7 NUAK2 NEK8 PAN3 PASK PKN1 OXSR1 PLK1 PLK1 PRKDC RIPK3 SMG1 SRPK1 PRP4B ROCK1 STK3 STK38 ST38L STK10 STK4 TLK1 TLK2 ULK3 VRK1 WNK1 YES TITIN
I10
L20
J4
12
3
6
34
7
18
19
KEGG pathway enrichment analysis of DTEP associated protein kinase
cell cycle
mTOR signaling pathway
p53 signaling pathway
NF-kappa B signaling pathway
MAPK signaling pathway
Insulin resistance
Neutrophin signaling pathway
Epstein-Barr virus infection
viral carcinogenesis
PI3K-Akt signaling pathway
% Gene Set
-log (p value)

Figure S1 (related to Figure 1). Phenotypes of ABT-199 (Venetoclax) Resistant Mantle Cell Lymphoma

(A) Representative images of parental HBL-2 mantle cell lymphoma cells (left), and the evolution of DTP (middle) and DTEP cells (right) following treatment with ABT-199. Following extended drug withdrawal the phenotype of subpopulations of DTEP can revert to become drug sensitive.

(B) Dose responses of parental HBL-2 cells (left panel), DTEP L20, J4, and I10 cells (middle panel) and "drug holiday" DTEP clones (dh, right panel) at 72 hr ABT-199 treatment.

(C) DTEP cells have increased sensitivity to the MCL-1 inhibitor S63845 versus HBL-2 parental cells as shown by S63845 dose response (left panel, 72 hr treatment) and time response (right panel, 0.12 μm S63845) curves.

(D) Top, ABPP kinome profiling (Log2 fold change) of DTEP cells compared with parental cells. Log2 Fold Change ≥1 indicates increased kinase ATP probe binding. Data shown as means of three biological replicates. Lower left, Venn diagram showing overlapped and shared kinases among the three DTEP cells when compared with kinases of parental HBL-2 cells. Lower right, KEGG pathway analysis of DTEP-associated up-regulated kinases (1.5 fold in at least 2 of 3 DTEP cells) showing signaling pathways activated in DTEP cells.

(B, C) A representative experiment (in triplicate) of at least 3 independent experiments is shown.

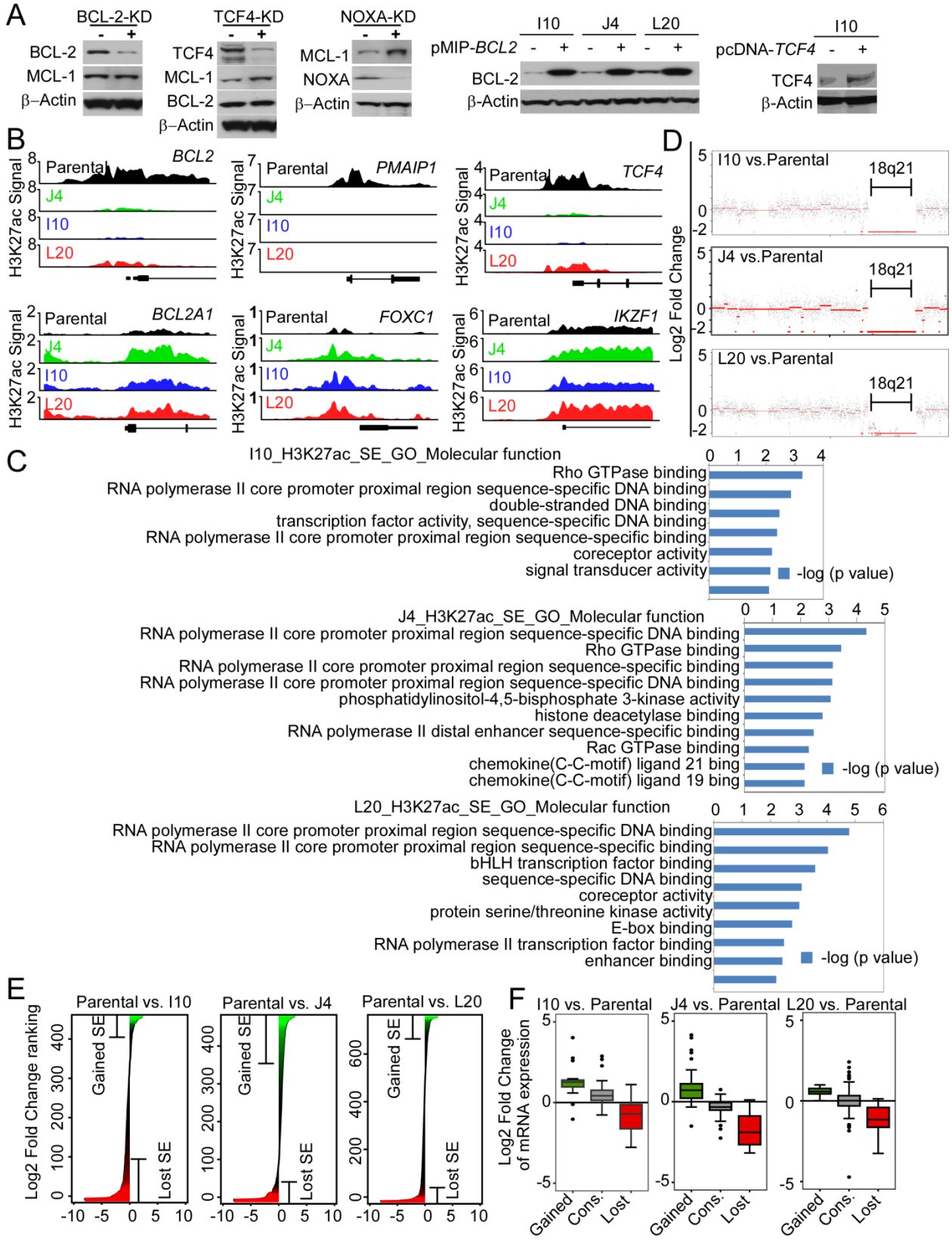
A
BCL-2-KD
TCF4-KD
NOXA-KD
BCL-2
MCL-1
β–Actin
TCF4
MCL-1
BCL-2
β–Actin
MCL-1
NOXA
β–Actin
I10
J4
L20
pMIP-BCL2
BCL-2
β-Actin
I10
pcDNA-TCF4
TCF4
β-Actin
B
H3K27ac Signal
Parental
J4
I10
L20
BCL2
PMAIP1
TCF4
BCL2A1
FOXC1
IKZF1
D
Log2 Fold Change
I10 vs.Parental
J4 vs.Parental
L20 vs.Parental
18q21
C
I10_H3K27ac_SE_GO_Molecular function
Rho GTPase binding
RNA polymerase II core promoter proximal region sequence-specific DNA binding
double-stranded DNA binding
transcription factor activity, sequence-specific DNA binding
RNA polymerase II core promoter proximal region sequence-specific binding
coreceptor activity
signal transducer activity
-log (p value)
J4_H3K27ac_SE_GO_Molecular function
RNA polymerase II core promoter proximal region sequence-specific DNA binding
Rho GTPase binding
RNA polymerase II core promoter proximal region sequence-specific binding
RNA polymerase II core promoter proximal region sequence-specific DNA binding
phosphatidylinositol-4,5-bisphosphate 3-kinase activity
histone deacetylase binding
RNA polymerase II distal enhancer sequence-specific binding
Rac GTPase binding
chemokine(C-C-motif) ligand 21 bing
chemokine(C-C-motif) ligand 19 bing
-log (p value)
L20_H3K27ac_SE_GO_Molecular function
RNA polymerase II core promoter proximal region sequence-specific DNA binding
RNA polymerase II core promoter proximal region sequence-specific binding
bHLH transcription factor binding
sequence-specific DNA binding
coreceptor activity
protein serine/threonine kinase activity
E-box binding
RNA polymerase II transcription factor binding
enhancer binding
-log (p value)
E
Parental vs. I10
Parental vs. J4
Parental vs. L20
Log2 Fold Change ranking
Gained SE
Lost SE
F
I10 vs. Parental
J4 vs. Parental
L20 vs. Parental
Log2 Fold Change of mRNA expression
Gained
Cons.
Lost

Figure S2 (related to Figure 2). 18q21 Amplicon Loss and Super-Enhancer Remodeling Drive ABT-199 Resistance in Mantle Cell Lymphoma

(A) Western blots showing CRISPR-Cas9-mediated knockdown (KD) of BCL2, NOXA and TCF4 in parental HBL-2 cells (first three panels to the left), and overexpression of BCL2 or TCF4 (two right panels) in the indicated DTEP cells.

(B) H3K27ac ChIP-Seq occupancy profiles at the *BCL2*, *PMAIP1*, *BCL2A1*, *TCF4*, *FOXC1* and *IKZF1* genes in parental and DTEP cells.

(C) Gene ontology (GO) analysis of the H3K27ac-identified SEs in DTEP cells. Bars indicate statistical significance shown as -log (p value).

(D) H3K27ac ChIP-seq signals for chromosome 18 in DTEPs compared to parental cells.

(E) All genomic regions containing gained or lost SEs in three DTEP clones compared to parental cells, ranked by Log2 fold change in H3K27ac signals (parental versus DTEP). The x axis shows the Log2 fold change of parental versus DTEPs in H3K27ac signals. Changes of H3K27ac intensity levels are colored in green (high in DTEP) to red (high in parental).

(F) Box plots showing Log2 fold changes in gene expression of DTEP cells compared to parental cells that are regulated by gained, lost or conserved (cons.) SEs. Top, middle, and bottom lines of the box plot represent third quantile, median and first quantile of all values, respectively. The whiskers represent the highest and lowest observations excluding the possible outliers. Gained or lost SE-associated genes are those genes with H3K27ac signal enrichment exhibiting a greater or less than 2 fold enrichment in DTEPs versus parental cells. Significance was determined using the Kruskal-Walllis test; I10, $p = 6.5e-16$; J4, $p < 2.2e-16$; L20, $p = 4.3e-9$.

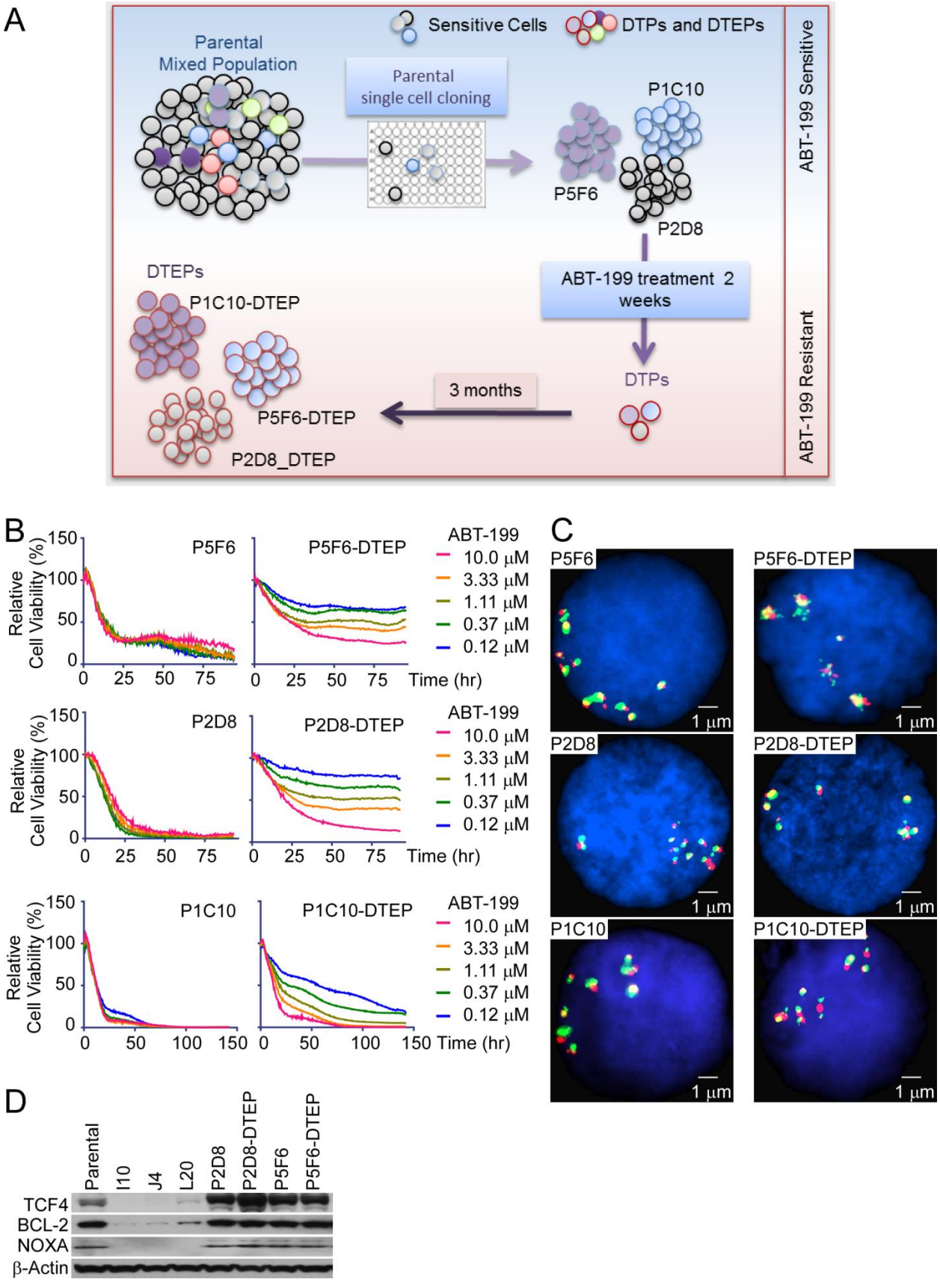
A
Sensitive Cells
DTPs and DTEPs
Parental
Mixed Population
Parental
single cell cloning
P1C10
P5F6
P2D8
ABT-199 Sensitive
ABT-199 treatment 2
weeks
DTPs
DTEPs
P1C10-DTEP
P5F6-DTEP
P2D8_DTEP
3 months
ABT-199 Resistant
B
P5F6
P5F6-DTEP
P2D8
P2D8-DTEP
P1C10
P1C10-DTEP
Relative
Cell Viability (%)
Time (hr)
ABT-199
10.0 μM
3.33 μM
1.11 μM
0.37 μM
0.12 μM
C
P5F6
P5F6-DTEP
P2D8
P2D8-DTEP
P1C10
P1C10-DTEP
1 μm
D
Parental
I10
J4
L20
P2D8
P2D8-DTEP
P5F6
P5F6-DTEP
TCF4
BCL-2
NOXA
β-Actin

Figure S3 (related to Figure 2). Characterization of Single Cell-Derived ABT-199 DTEPs

(A) Schematic overview of experimental design for establishment of single cell-derived "acquired" drug-tolerant expanded persisters (DTEP) from parental HBL-2 MCL cells. See STAR Methods for details.

(B) Image-based cell viability assays showing ABT-199 response of three pairs of the indicated single cell parental (left) and single cell-derived "acquired" DTEP (right) cells.

(C) Fluorescence in situ hybridization (FISH) analysis using a *BCL2* probe at the18q21 locus in single cell parental (left) and their paired single-cell acquired DTEP (right) cells. Cell nuclei are counterstained with DAPI in blue, 5' region of *BCL2* gene was targeted with red colored probe and 3' region of *BCL2* gene with green colored probe. One isolated fusion signal represents one normal *BCL2* gene while other *BCL2* fusion signals in cluster indicate *BCL2* gene amplification.

(D) Western blot analyses of BCL-2, TCF4 and NOXA protein levels in ABT-199-sensisitve HBL-2 (parental, P2D8, P5F6) cells, in bulk population-selected DTEP variants (I10, J4, L20) and in single-cell acquired DTEP cells (P2D8-DTEP, P5F6-DTEP). Data are representatives of 3 independent experiments.

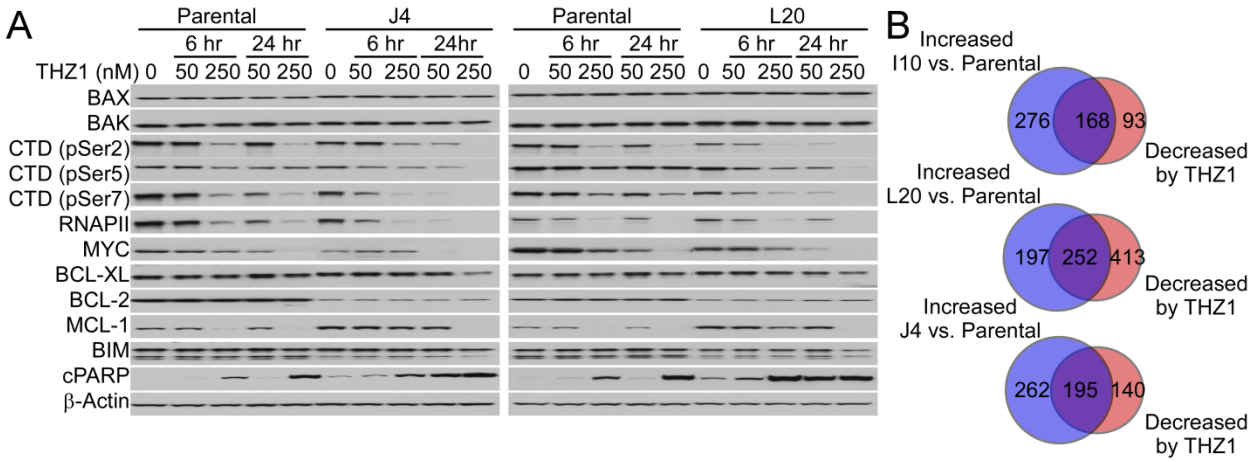
A
Parental
J4
Parental
L20
6 hr
24 hr
6 hr
24hr
6 hr
24 hr
6 hr
24 hr
THZ1 (nM) 0 50 250 50 250 0 50 250 50 250 0 50 250 50 250 0 50 250 50 250
BAX
BAK
CTD (pSer2)
CTD (pSer5)
CTD (pSer7)
RNAPII
MYC
BCL-XL
BCL-2
MCL-1
BIM
cPARP
β-Actin
B
Increased I10 vs. Parental
276
168
93
Decreased by THZ1
Increased L20 vs. Parental
197
252
413
Decreased by THZ1
Increased J4 vs. Parental
262
195
140
Decreased by THZ1

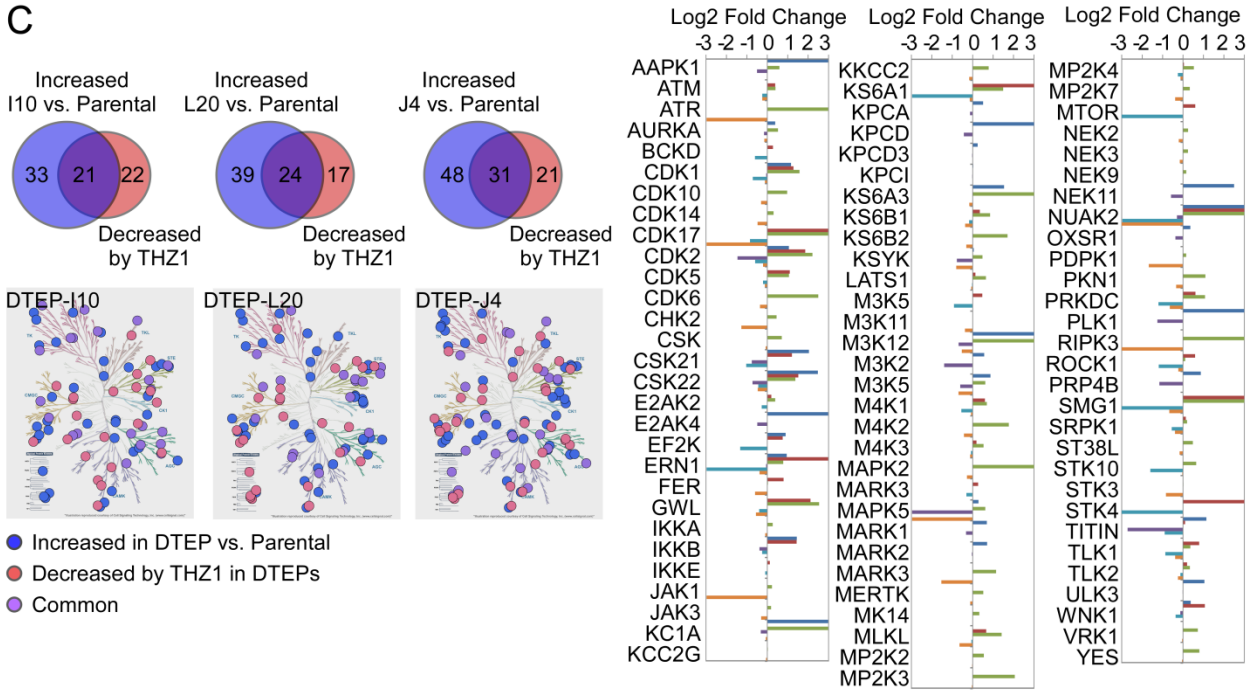
C
Increased I10 vs. Parental
33
21
22
Decreased by THZ1
Increased L20 vs. Parental
39
24
17
Decreased by THZ1
Increased J4 vs. Parental
48
31
21
Decreased by THZ1
DTEP-I10
DTEP-L20
DTEP-J4
Increased in DTEP vs. Parental
Decreased by THZ1 in DTEPs
Common
Log2 Fold Change
-3 -2 -1 0 1 2 3
AAPK1
ATM
ATR
AURKA
BCKD
CDK1
CDK10
CDK14
CDK17
CDK2
CDK5
CDK6
CHK2
CSK
CSK21
CSK22
E2AK2
E2AK4
EF2K
ERN1
FER
GWL
IKKA
IKKB
IKKE
JAK1
JAK3
KC1A
KCC2G
KKCC2
KS6A1
KPCA
KPCD
KPCD3
KPCI
KS6A3
KS6B1
KS6B2
KSYK
LATS1
M3K5
M3K11
M3K12
M3K2
M3K5
M4K1
M4K2
M4K3
MAPK2
MARK3
MAPK5
MARK1
MARK2
MARK3
MERTK
MK14
MLKL
MP2K2
MP2K3
MP2K4
MP2K7
MTOR
NEK2
NEK3
NEK9
NEK11
NUAK2
OXSR1
PDPK1
PKN1
PRKDC
PLK1
RIPK3
ROCK1
PRP4B
SMG1
SRPK1
ST38L
STK10
STK3
STK4
TITIN
TLK1
TLK2
ULK3
WNK1
VRK1
YES

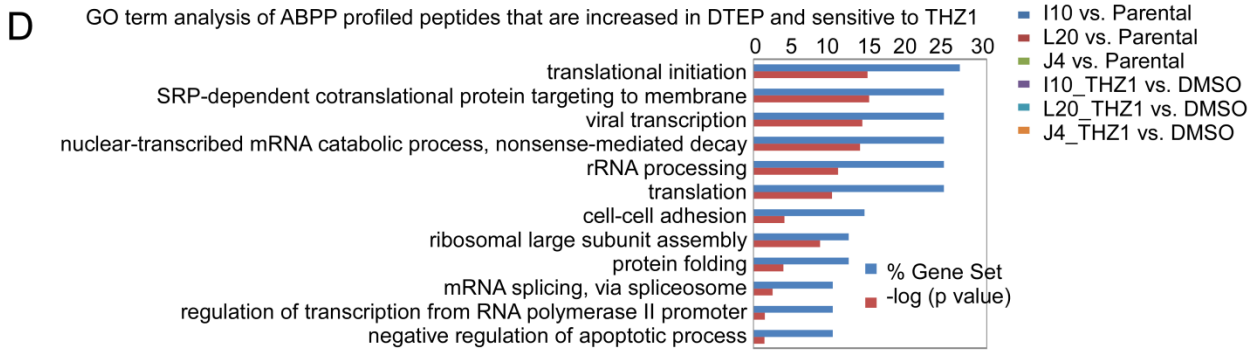
D
GO term analysis of ABPP profiled peptides that are increased in DTEP and sensitive to THZ1
0 5 10 15 20 25 30
translational initiation
SRP-dependent cotranslational protein targeting to membrane
viral transcription
nuclear-transcribed mRNA catabolic process, nonsense-mediated decay
rRNA processing
translation
cell-cell adhesion
ribosomal large subunit assembly
protein folding
mRNA splicing, via spliceosome
regulation of transcription from RNA polymerase II promoter
negative regulation of apoptotic process
% Gene Set
-log (p value)
I10 vs. Parental
L20 vs. Parental
J4 vs. Parental
I10_THZ1 vs. DMSO
L20_THZ1 vs. DMSO
J4_THZ1 vs. DMSO

Figure S4 (related to Figure 3). ABT-199 Resistant DTEP Cells Are Preferentially Sensitive to CDK7 Inhibition

(A) Western blots of parental HBL-2 and DTEP cells treated with the indicated doses of THZ1 at different time points. CTD, C-terminal repeat domain of RNAPII; cPARP, cleaved PARP. Data shown are representative of at least 3 independent experiments.

(B) Venn diagrams of significantly up-regulated (> 1.5-fold) ABPP binding peptides in DTEP cells versus parental cells and down-regulated peptides peptides following THZ1 treatment in DTEP cells (50 nM, 6 hr).

(C) Kinases differentially expressed in DTEP cells compared to parental cells and kinases down regulated by THZ1 in DTEP cells. Top left, Venn diagrams of kinases that were selectively up-regulated (>1.5-fold) in DTEP cells and that were down-regulated (>1.5-fold) by THZ1 treatment in DTEP cells (50 nM, 6 hr). Bottom left, kinome tree representation of kinases whose activity was significantly up-regulated (blue circles) in DTEP cells compared to parental cells or reduced (red circles) in DTEP cells by THZ1 treatment. Kinases that overlap between these two groups are indicated by purple circles. Right, Log2 fold change in the activity of the indicated kinases in DETP cells versus parental cells or between THZ1 treatment and DMSO in DTEP cells is shown for the indicated kinases.

(D) GO (Gene Ontology) term analysis of DTEP-upregulated (in all 3 DTEP cells) and THZ1-sensitive (decreased by THZ1 treatment at 50 nM for 6 hr) ABPP profiled peptides.

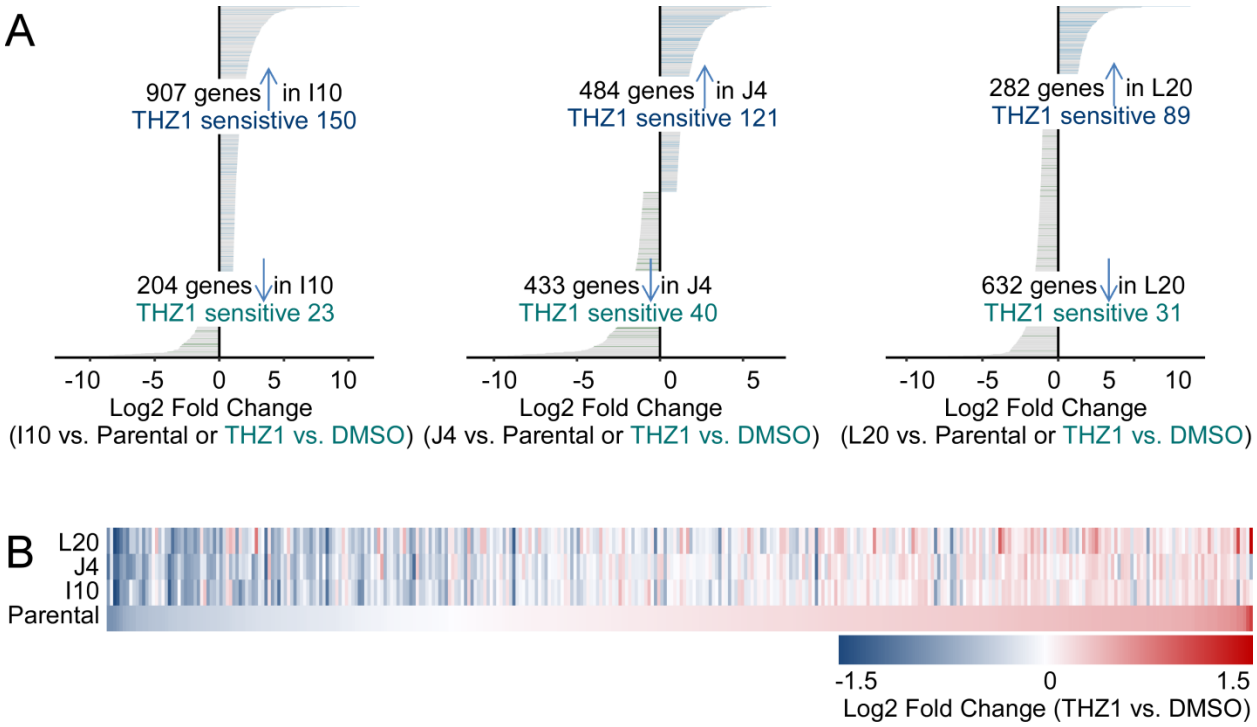

Figure S5 (related to Figure 4). CDK7 Inhibition Suppresses SE-Driven Transcriptional Reprogramming, and Overcomes and Blocks the Evolution of ABT-199 Drug Resistance

(A) DTEP up-regulated genes are suppressed by THZ1 treatment. Log2 fold changes in gene expression in DTEP versus parental HBL-2 cells are shown along the x axis. Genes differentially expressed in DTEP cells relative to parental cells were identified as 'DTEP-specific' (right side of y axis). Among DTEP-specific genes, genes whose expression decreased by 1.2-fold or greater upon treatment with THZ1 (colored) were identified as DTEP-specific/THZ1-sensitive genes.

(B) Heatmap of DTEP-specific/THZ1-sensitive genes shows average changes after 6 hr treatment with THZ1 (50 nM), respectively, in parental and DTEP cells. Color represents Log2 fold changes in gene expression, where the scale ranges from the minimum to the maximum value observed in parental cells.

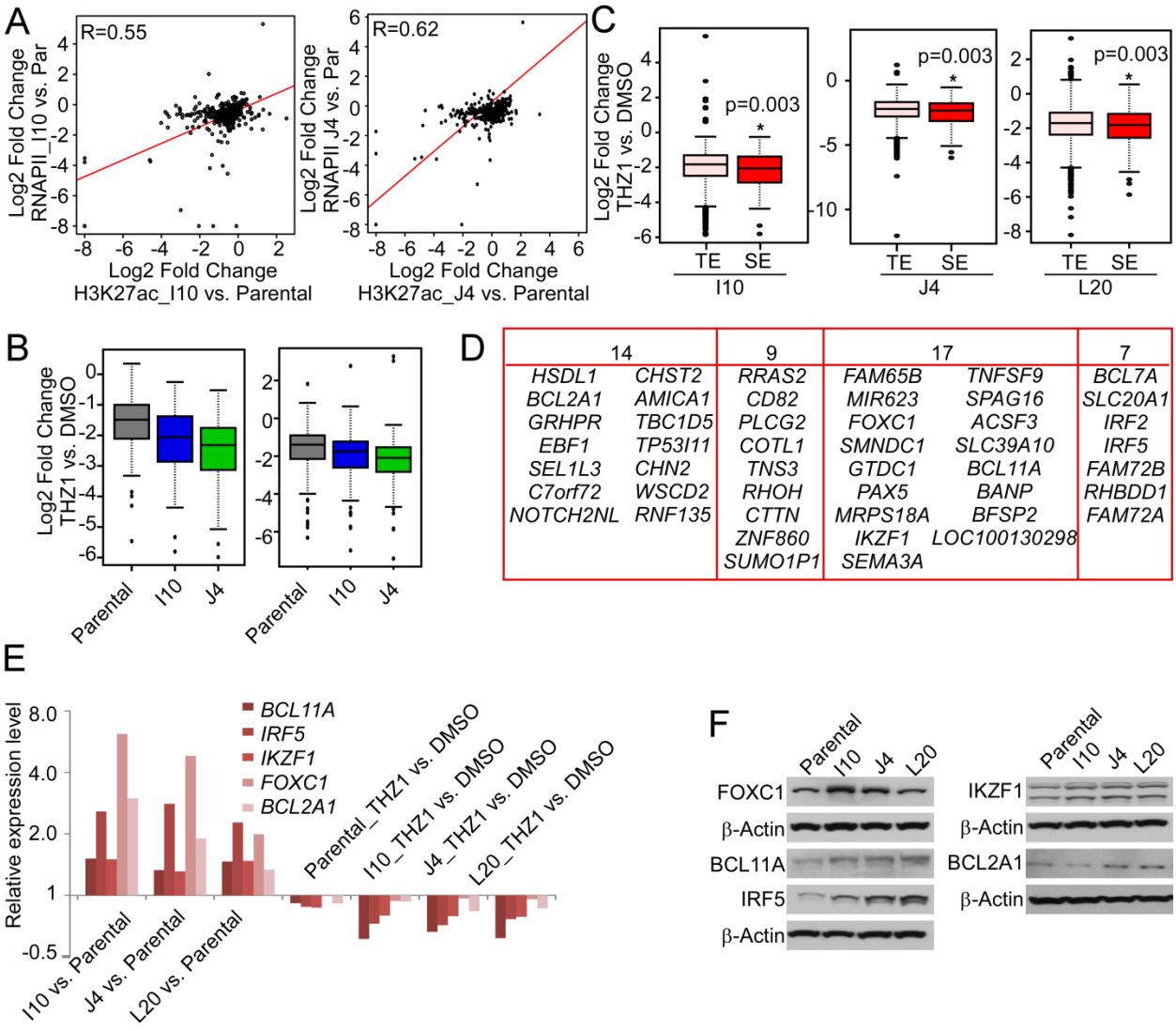

Figure S6 (related to Figure 5). Super-Enhancer Remodeling Contributes to Preferential Sensitivity to CDK 7 Inhibition in ABT-199 DTEP Cells

(A) Correlations of Log2 fold changes in H3K27ac and pRNAPII obtained by ChIP-seq of I10 and J4 DTEP versus parental HBL-2 cells. The coefficient of determination (R) was calculated using a simple linear regression model.

(B) Box plots of Log2 fold change of gene expression in parental, I10 and J4 by THZ1 treatment (50 nM, 6 hr). Left, gained H3K27ac-bound SEs regulated genes; right, pRNAPII SE occupied genes. Top, middle, and bottom lines of the box plot represent third quantile, median and first quantile of all values, respectively. The whiskers represent the highest and lowest observations excluding the outliers.

(C) Box plots of of Log2 fold changes in the expression of genes that regulated by typical enhancer (TE) or super enhancer (SE) in I10, J4 and L20 by THZ1 treatment (50 nM, 6 hr). Top, middle, and bottom lines of the box plot represent third quantile, median and first quantile of all

values, respectively. The whiskers represent the highest and lowest observations excluding the possible outliers.
(D) List of top SE-associated/THZ1-sensitive transcripts in DTEP cells.
(E) Relative expression of the indicated SE-associated/THZ1-sensitive genes in parental versus DTEP cells (mean ± SD, n=3), and in the indicated cells ± THZ1 treatment (50 nM, 6 hr, n=3).
(F) Expression of SE-associated/THZ1-sensitive proteins was assessed in the indicated cells by western blot.
(E, F) Data shown are representative of at least two independent experiments.

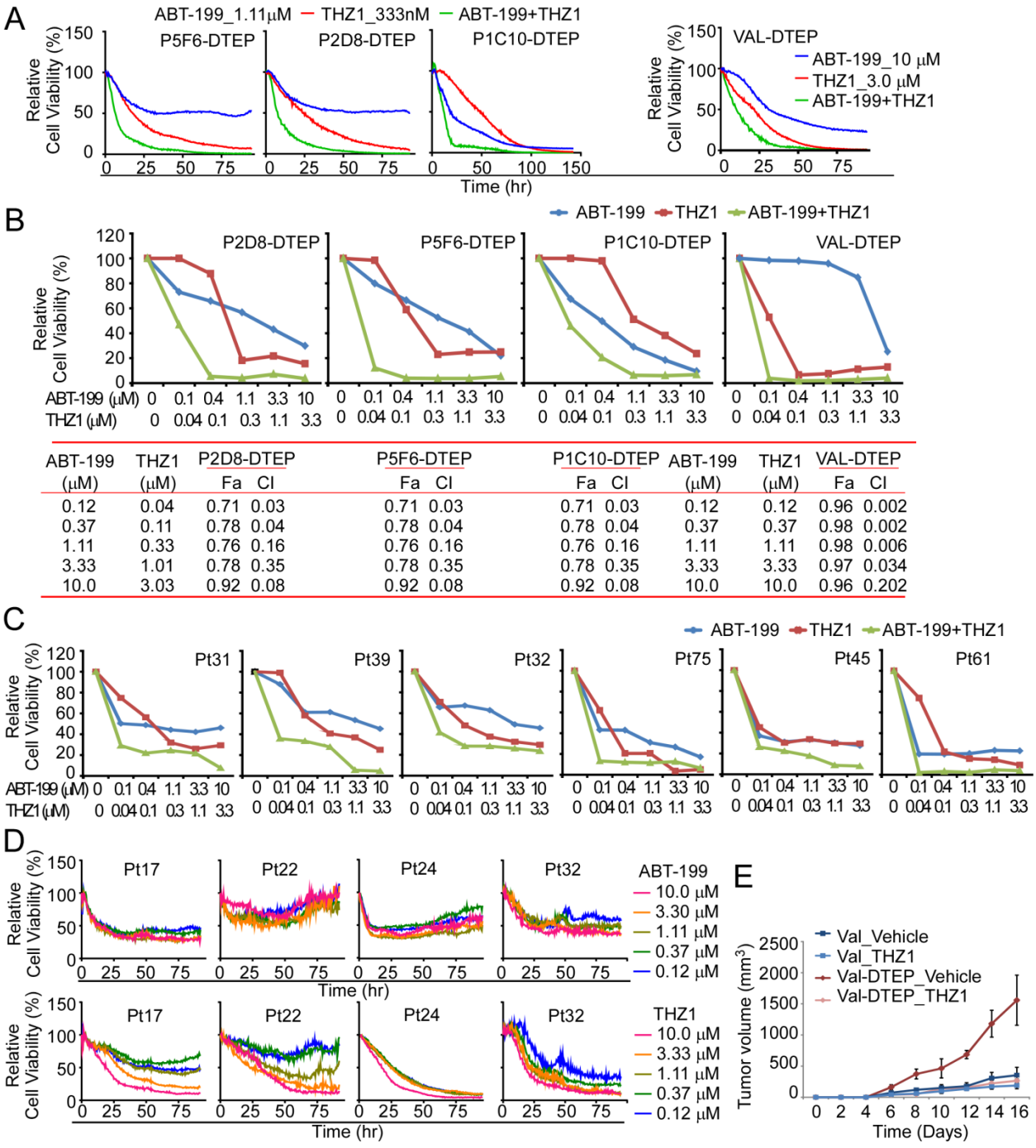

ABT-199 (μM)	THZ1 (μM)	P2D8-DTEP Fa	P2D8-DTEP CI	P5F6-DTEP Fa	P5F6-DTEP CI	P1C10-DTEP Fa	P1C10-DTEP CI	ABT-199 (μM)	THZ1 (μM)	VAL-DTEP Fa	VAL-DTEP CI
0.12	0.04	0.71	0.03	0.71	0.03	0.71	0.03	0.12	0.12	0.96	0.002
0.37	0.11	0.78	0.04	0.78	0.04	0.78	0.04	0.37	0.37	0.98	0.002
1.11	0.33	0.76	0.16	0.76	0.16	0.76	0.16	1.11	1.11	0.98	0.006
3.33	1.01	0.78	0.35	0.78	0.35	0.78	0.35	3.33	3.33	0.97	0.034
10.0	3.03	0.92	0.08	0.92	0.08	0.92	0.08	10.0	10.0	0.96	0.202

Figure S7 (related to Figure 7). CDK7 is a Vulnerability in MCL and DHL DTEP and ABT-199/THZ1 Synergy in Treatment of Mantle Cell Lymphoma and Double Hit Lymphoma

(A) Image-based viability assay of single cell-clone derived "acquired" DTEP (P5F6-DTEP, P2D8-DTEP, P1C10-DTEP) derived from HBL-2 MCL cells (left) and of DTEP cells derived from double hit lymphoma (DHL) VAL cells (VAL-DTEP, right) following treatment with the indicated concentrations of ABT-199, THZ1 or ABT-199+THZ1.

(B) Upper, mage-based cell viability of the indicated DTEP cells treated with different doses of ABT-199 and/or THZ1 (48 hr) on DTEP. Lower, combination index (CIs) for drug combinations were determined with CalcuSyn software using percent inhibition (fraction affected, Fa) resulting from combined action of the 2 drugs versus effects of either drug alone. CI values <1.0 indicate synergism of the 2 drugs.
(C) Image-based cell viability of primary MCL patient specimens treated with different doses of ABT-199 and/or THZ1 for 48 hr.
(D) Image-based cell viability of primary MCL patient specimens cultured on lymphoma stroma (HK stromal cells) cells following treatment with the indicated doses of ABT-199 or THZ1.
(E) Effect of THZ1 treatment on tumor growth of parental and VAL-DTEP xenografts in NOD/SCID recipient mice. n = 6 for each group. Data shown as mean ± SD.

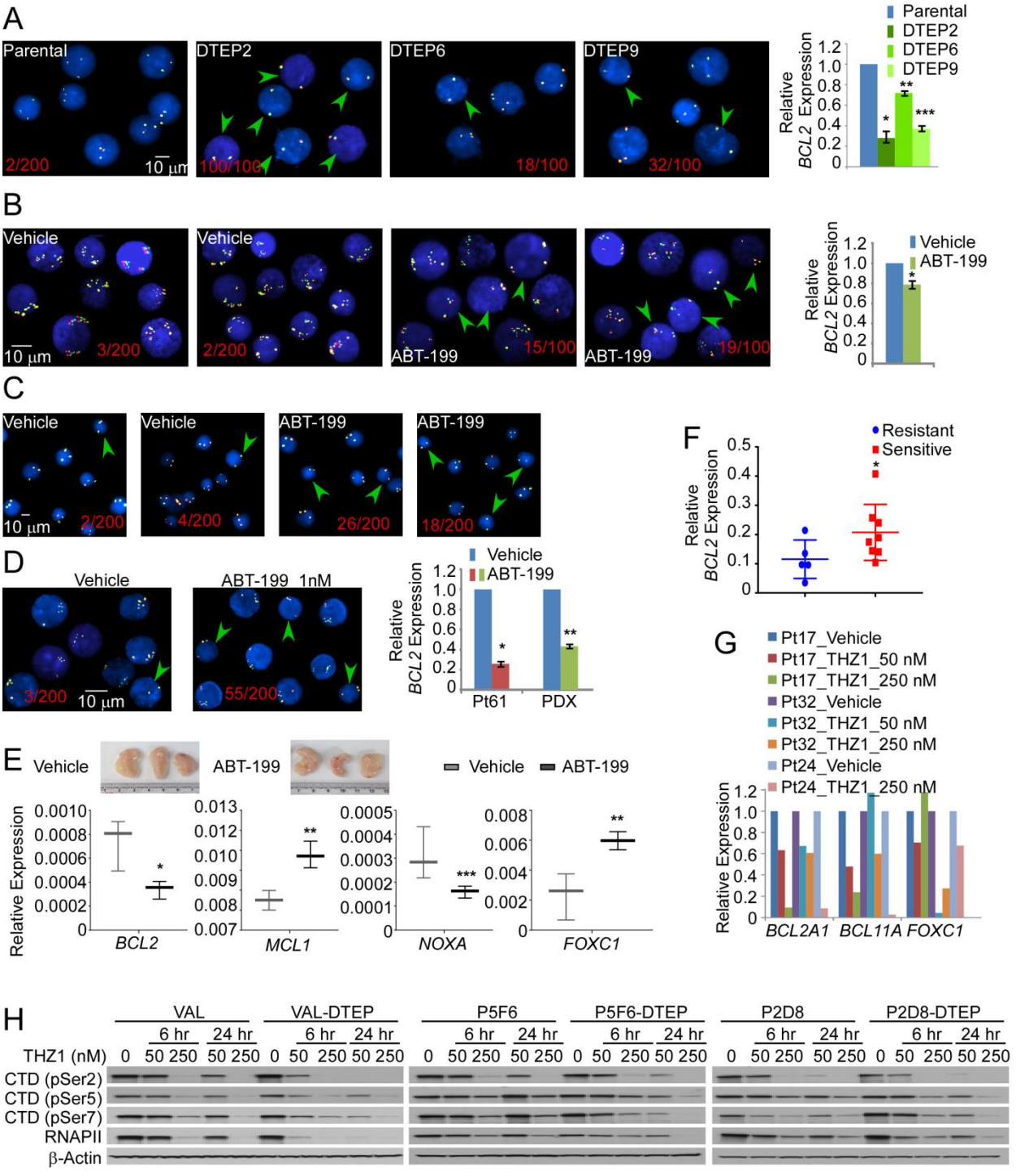

Figure S8 (related to Figure 7). Selection for *BCL2* Amplicon Loss and CDK7 Vulnerability Are Hallmarks of ABT-199-Resistant MCL, DHL and Primary MCL Patient Samples.

(A) Left, FISH analysis using a *BCL2* probe in parental and DTEP Mino MCL cells. The numbers in red represent the percentage of cells with 18q21 loss; the green arrows point cells with 18q21 loss. Right, relative expression of *BCL2* determined by qRT-PCR. Data are shown as mean ± SD

and analyzed by unpaired Student's t-test, *p=0.006, **p=0.013, ***p=0.003. (A-D), Cell nuclei are counterstained with DAPI in blue, 5' region of *BCL2* gene was targeted with red colored probe and 3' region of *BCL2* gene with green colored probe. One isolated fusion signal represents one normal *BCL2* gene while other *BCL2* fusion signals in cluster indicate *BCL2* gene amplification.

(B) Left panels, FISH analyses using a *BCL2* probe of tumors from vehicle or ABT-199 treated (5 mg/kg daily for 10 days) NOD/SCID recipient mice bearing HBL-2 MCL xenografts. Right, relative expression of *BCL2* in tumors determined by qRT-PCR. Data are shown as mean ± SD and analyzed by unpaired Student's t-test, *p=0.032).

(C) FISH analyses using a *BCL2* probe of tumors from vehicle or ABT-199 treated (5 mg/kg daily for 14 days) NSG recipient mice bearing a DHL PDX model.

(D) Left, FISH analyses using a *BCL2* probe of surviving cells from a primary MCL patient sample that has the 18q21 amplicon following treatment (48 hr) with 1 nM ABT-199. Right, relative expression of *BCL2* in a primary MCL lymphoma and a DHL PDX determined by qRT-PCR. Data are shown as mean ± SD and analyzed by unpaired Student's t-test was used, *p=0.002, **p=0.009,***p=0.05. Cell nuclei are counterstained with DAPI in blue, 5' region of BCL2 gene was targeted with red colored probe and 3' region of BCL2 gene with green colored probe. One isolated fusion signal represents one normal BCL2 gene while five BCL2 fusion signals in cluster indicate BCL2 gene amplification (oval circle) (A-D).

(E) Representative images of tumors (upper) and relative expression of *BCL2, NOXA*, *MCL1* and *FOXC1* (lower) in vehicle versus ABT-199 (5 mg/kg daily) treated NOD/SCID recipient mice bearing VAL DHL xenografts. Data shown as mean ± SD (n=3 for each cohort) and analyzed by unpaired Student's t-test, *p=0.04, **p=0.004.

(F) Relative expression of *BCL2* in 13 primary MCL patient samples determined by qRT-PCR. Their sensitivity to ABT-199 was determined using image-based viability analyses. Data shown are representative of 3 independent experiments, *p=0.045 by Mann-Whitney *U* test.

(G) Expression of the SE-associated, THZ1-sensitive genes *BCL2A1*, *BCL11A*, and *FOXC1* in 3 primary MCL patient specimens that were treated with 50 nM or 250 nM of THZ1 (6 hr) determined by qRT-PCR.

(H) Western blots of the indicated parental and DTEP cells treated with different doses of THZ1 at the indicated time points. Data shown are representative of 3 independent experiments.